Persistent and Transient Open-Shell Species Derived from C_{60}−TTF Cyclohexene-Fused Dyads

Josep Llacay,[†] Jaume Veciana,[†] José Vidal-Gancedo,[†] José Luis Bourdelande,[‡] Rafael González-Moreno,[‡] and Concepció Rovira*[,†]

Institut de Ciència de Materials de Barcelona (CSIC), Campus UAB, E-08913 Bellaterra, Spain, and Departament de Química, Unitat de Química Orgànica, Universitat Autònoma de Barcelona, Campus UAB, E-08913 Bellaterra, Spain

Received March 17, 1998

A new series of donor−acceptor fused dyads consisting of a C_{60} doubly tethered to a substituted TTF moiety has been synthesized. Cyclic voltammetry of the new fullerene derivatives in solution shows a modulation in the difference between the first reduction potential of the fullerene moiety and the first oxidation potential of the TTF moiety with the substituents of the TTF addend. Along with the neutral bichromophoric compounds, we also report the generation and characterization by EPR and absorption spectroscopies of the corresponding persistent open-shell species obtained electrochemically, namely their radical cations and radical anions. Spin density distributions of radical cations and radical anions derived from dyads **1a**−**c** are mainly located on the TTF and fullerene moieties, respectively, as ascertained from the *g* values and ^{33}S hyperfine coupling constants. Interestingly, the EPR of the radical anion derived from the bisadduct **1d** exhibits a structured signal ($g = 2.0005$) arising from the coupling of the unpaired electron with the hydrogen atoms of the addends. The modification of the donor strength of the TTF moiety allows the tuning of the HOMO−LUMO gap of dyads, permitting a study of the interaction between the two electroactive centers of the molecules as a function of the donor strength. Nanosecond-resolved flash photolysis in the UV−vis region of dyads **1a**−**c** in degassed benzonitrile shows a rapid quenching of the corresponding excited triplet states, which indicates different lifetimes depending on the donor ability of their TTF addends. Excited triplet states of **1b** and **1c** evolve toward transient charge-separated open-shell species that have remarkably long lifetimes (**1b**, $\tau = 75 \times 10^{-6}$ s; **1c**, $\tau = 79 \times 10^{-6}$ s) and show absorptions around 460 and 620 nm due to the radical cation on the TTF moiety. These biradical species are also observed by LESR, having in frozen solution spectra consistent with strong exchange coupling between both electrons.

Introduction

Since the discovery of a facile method for the synthesis in gram quantities of fullerenes,[1] the availability of these appealing molecules has allowed the exploration and development of their chemistry. It has been established by cyclic voltammetry that C_{60} is a moderately good electron acceptor able to accept up to six electrons in its LUMO.[2] This behavior, along with the possibility of linking a functional group to its carbon framework, through a great variety of cycloaddition reactions, without altering its electron-acceptor properties, has made C_{60} a very interesting molecule to build up novel molecular materials with remarkable electronic, magnetic, or biological properties. Up to now, several electron-donor fragments have been attached to the C_{60} cage,[3−8] and in some cases, the final bichromophoric compounds show interesting intramolecular electronic interactions between the fullerene moiety and the addend.[4] Some of these donor−acceptor dyads form long-lived charge-separated species upon irradiation,[5−8] being interesting systems as molecular building blocks in electrooptical devices and also bistable molecular information storage units. It is remarkable that C_{60} as acceptor in electron-transfer processes accelerates photoinduced charge separation and shows a slow charge recombination in the dark.[4,8] This feature makes the photoinduced charge

[†] Institut de Ciència de Materials de Barcelona.

[‡] Departament de Química, Unitat de Quimica Orgànica.

(1) Krästchmer, W.; Lamb, L. D.; Fostiropoulos, K.; Huffman, D. R. *Nature* **1990**, *347*, 354.

(2) Xie, Q.; Pérez-Cordero, E.; Echegoyen, L. *J. Am. Chem. Soc.* **1992**, *114*, 3978.

(3) (a) Prato, M. *J. Mater. Chem.* **1997**, *7*, 1097. (b) Rubin, Y.; Khan, S.; Freedberg, D. I.; Yeretzian, C. *J. Am. Chem. Soc.* **1993**, *115*, 344. (c) Rubin, Y.; Khan, S. I.; Oliver, A. M.; Paddon-Row, M. N. *Ibid.* **1993**, *115*, 4919. (d) Mullen, K.; Belik, P.; Gügel, A.; Spickermann, J. *Angew. Chem., Int. Ed. Engl.* **1993**, *32*, 78. (e) Liddell, P.; Mcpherson, A. N.; Sumida, J.; Demanche, L.; Moore, A. L.; Moore, T. A.; Gust, D. *Photochem, Photobiol.* **1994**, *595*, 365. (f) Linssen, T. G.; Dürr, K.; Hanack, M.; Hirsch, A. *J. Chem. Soc., Chem. Commun.* **1995**, 103.

(4) Matsubara, Y.; Tada, H.; Nagase, S.; Yoshida, Z. *J. Org. Chem.* **1995**, *60*, 5372.

(5) (a) Lawson, J. M.; Oliver, A. M.; Rothenfluh, D. F.; An, Y.-Z.; Ellis, G. A.; Ranasinghe, M. G.; Khan, S. I.; Franz, A. G.; Ganapathi, P. S.; Shephard, M. J.; Paddon-Row, M. N.; Rubin, Y. *J. Org.Chem.* **1996**, *61*, 5032. (b) Williams, R. M.; Koeberg, M.; Lawson, J. M.; An, Y.-Z.; Rubin. Y.; Paddon-Row, M. N.; Verhoeven, J. W. *Ibid.* **1996**, *61*, 5055. (c) Williams, R. M.; Zwier, J. M.; Verhoeven, J. W. *J. Am. Chem. Soc.* **1995**, *117*, 4093.

(6) (a) Kuciauskas, S.; Lin, S.; Seely, G. R.; Moore, A. L.; Moore, T. A.; Gust, D.; Drovetskaya, T.; Reed, C. A.; Boyd, P. D. W. *J. Phys. Chem.* **1996**, *100*, 15926. (b) Liddell, P. A.; Kuciauskas, S.; Sumida, J. P.; Nash, B.; Nguyen, D.; Moore, A. L.; Moore, T. A.; Gust, D. *J. Am. Chem. Soc.* **1997**, *119*, 1400.

(7) (a) Sariciftci, N. S.; Wudl, F.; Heeger, A. J.; Maggini, M.; Scorrano, G.; Prato, M. Bourassa, J.; Ford, P. C. *Chem. Phys. Lett.* **1995**, *247*, 510. (b) Guldi, D. M.; Maggini, M.; Scorrano, G.; Prato, M. *J. Am. Chem. Soc.* **1997**, *119*, 974.

(8) (a) Imahori, H.; Hagiwara, K.; Aoki, M.; Akiyama, T.; Taniguchi, S.; Okada, T.; Shirakawa, M.; Sakata, Y. *J. Am. Chem. Soc.* **1996**, *118*, 11771. (b) Imahori, H.; Sakata, Y. *Adv. Mater.* **1997**, *9*, 537. (c) Sakata, Y.; Imahori, H.; Tsue, H.; Higashida, S.; Akiyama, T.; Yoshizawa, E.; Aoki, M.; Yamada, K.; Hagiwara, K.; Taniguchi, S.; Okada, T. *Pure Appl. Chem.* **1997**, *69*, 1951.

S0022-3263(98)00498-8 CCC: $15.00
Published on Web 07/08/1998

Chart 1

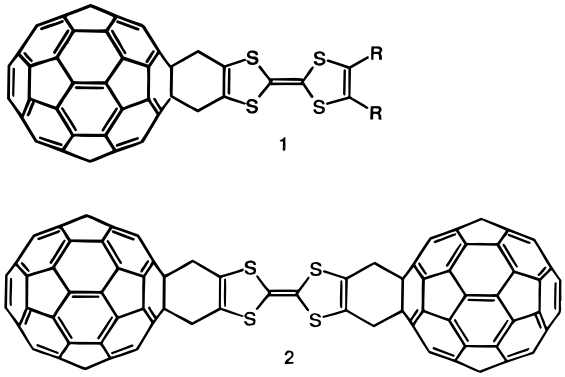

transfer in C_{60}−B−D dyads analogous to the electron transfer in the photosynthetic reaction center.

The well-known donor tetrathiafulvalene (TTF) and its derivatives,[9] which give rise to metallic charge-transfer complexes with strong electron acceptors such as, for example, tetracyano-*p*-quinodimethane (TCNQ), also form charge-transfer complexes with C_{60} having small or negligible degrees of charge transfer.[11−13] TTF derivatives have also been covalently linked to C_{60} through a flexible pyrrolidine bridge forming donor−acceptor dyads.[14,15] Nevertheless, in the resulting systems, no electronic interactions between the donor and acceptor centers have been reported. The absence of electronic interactions in the latter compounds is probably due to the large distance between the redox active centers and the relatively flexible bridge between them. To promote such electronic interactions, we have adopted a different strategy consisting of the linking of C_{60} and TTF's by a rigid bridge. So, C_{60}−TTF fused systems have been designed in such a way that the C_{60} acceptor and the TTF donor are directly attached by two rigid σ bonds, forming a cyclohexene ring such as in **1** and **2** (Chart 1). The fusion of two electroactive centers with a six-membered ring provides not only a short distance, but also a rigid bridge between the donor and the acceptor, giving rise to a well-defined spacing and orientation with respect to each other. This kind of bridge has proven to be very efficient for mediating in electron- and energy-transfer between two electroactive centers by a through-bond coupling mechanism regardless of its length.[5] Moreover, the donor capacity of the TTF moiety can be modified by varying the nature of substituents R in the dyads **1**; this aspect provides the opportunity for a systematic study of the influence of the donor strength on the HOMO−LUMO gap and, as a consequence, on the efficiency of the intramolecular electron-transfer and on the charge-separation and charge-recombination processes.

Scheme 1

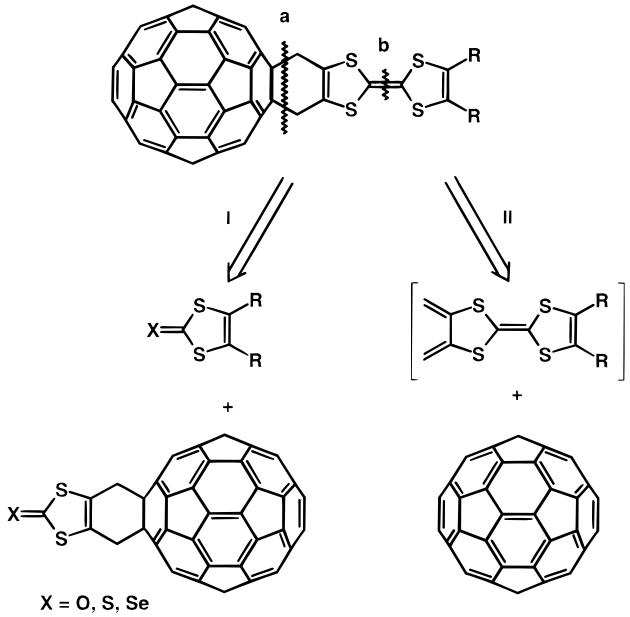

We herein report a detailed description of a synthetic pathway to obtain a new series of C_{60}−TTF dyads tethered by a cyclohexene ring,[16] as well as the formation and study of the stable and transient radical cations and radical anions derived from these bichromophoric systems. Studies by nanosecond-resolved flash photolysis in the UV−vis region and by light-induced electron-spin resonance (LEPR) show that the photoinduced intramolecular electron-transfer gives rise to remarkably long-lived transient charge-separated states in the dyads containing the addends with stronger electron-donor abilities, namely **1b** and **1c**. Moreover, these studies also show the first evidence of tuning the lifetimes of these transient species by modifying the donor ability of the TTF addend.

Results and Discussion

Synthesis and Characterization of Cycloadducts. The retrosynthetic analysis (Scheme 1) of the target structures **1** and **2** indicates the existence of two key bonds: (a) the two σ bonds between C_{60} and the TTF fragment and (b) the central double bond of the TTF core. The former bond can be made by a Diels−Alder cycloaddition since C_{60} is a good dienophile.[17] To build up the latter bond, many methodologies have been described.[18] Depending on the order of construction of these key bonds, there are two major approaches, as depicted in Scheme 1. One approach (route I) implies as a first step the formation of a C_{60} cycloadduct with a diene derivative bearing a dithiolium substituent able to be coupled to form the TTF skeleton. The second approach (route II) requires the synthesis of the TTF donor with a diene precursor functionalization first and its later cycloaddition to C_{60} through a Diels−Alder reaction.

To perform the cycloadditions to C_{60}, we have chosen precursors containing the sulfolene moiety, since this

(9) Williams, J. M.; Ferraro, J. R.; Thorn, R. J.; Carlson, K. D.; Geiser, U.; Wang, H. H.; Kini, A. M.; Whangbo, M.-H. *Organic Superconductors*; Prentice Hall: Englewood Cliffs, NJ, 1992.

(10) Izouka, A.; Tachikawa, T.; Sugawara, T.; Suzuki, Y.; Konno, M.; Saito, Y.; Shinohara, H. *J. Chem. Soc., Chem. Commun.* **1992**, 1472.

(11) Metzger, R. M.; Cava, M. P.; Shcherbakova, I.; Lee, W. J.; Wang, P. *Synth. Met.* **1994**, *64*, 319.

(12) Saito, G.; Teramoto, T.; Otsuka, A.; Sugita, Y.; Ban, T.; Kusunoki, M.; Sakagughi, K. *Synth. Met.* **1994**, *64*, 359.

(13) (a) Llacay, J.; Tarrés, J.; Veciana, J.; Rovira, C. *Synth. Met.* **1995**, *70*, 1453. (b) Llacay, J.; Mas, M.; Molins, E.; Rovira, C.; Veciana, J. *J. Phys. Chem. Solids* **1997,** *58*, 1675.

(14) Prato, M.; Maggini, M.; Giacometti, C.; Scorrano, G.; Sandonà, G.; Farina, G. *Tetrahedron* **1996**, *52*, 5221.

(15) (a) Martín, N.; Sánchez, L.; Seoane, C.; Andreu, R.; Garín, J.; Orduna, J. *Tetrahedron Lett.* **1996**, *37*, 5979. (b) Martín, N.; Pérez, I.; Sánchez, L.; Seoane, C. *J. Org. Chem.* **1997**, *62*, 5690.

(16) A preliminary account on the synthesis of the dyad **1a** and cycloadduct **4**, as well as on the crystal structure of last compound, has been recently published: Llacay, J.; Mas, M.; Molins, E.; Veciana, J.; Rovira, C. *Chem. Commun.* **1997**, 659.

(17) Hirsch, A. *The Chemistry of the Fullerenes*; Thieme: New York, 1994.

(18) Narita, M.; Pittman, C. U. *Synthesis* **1976**, 489.

Scheme 2

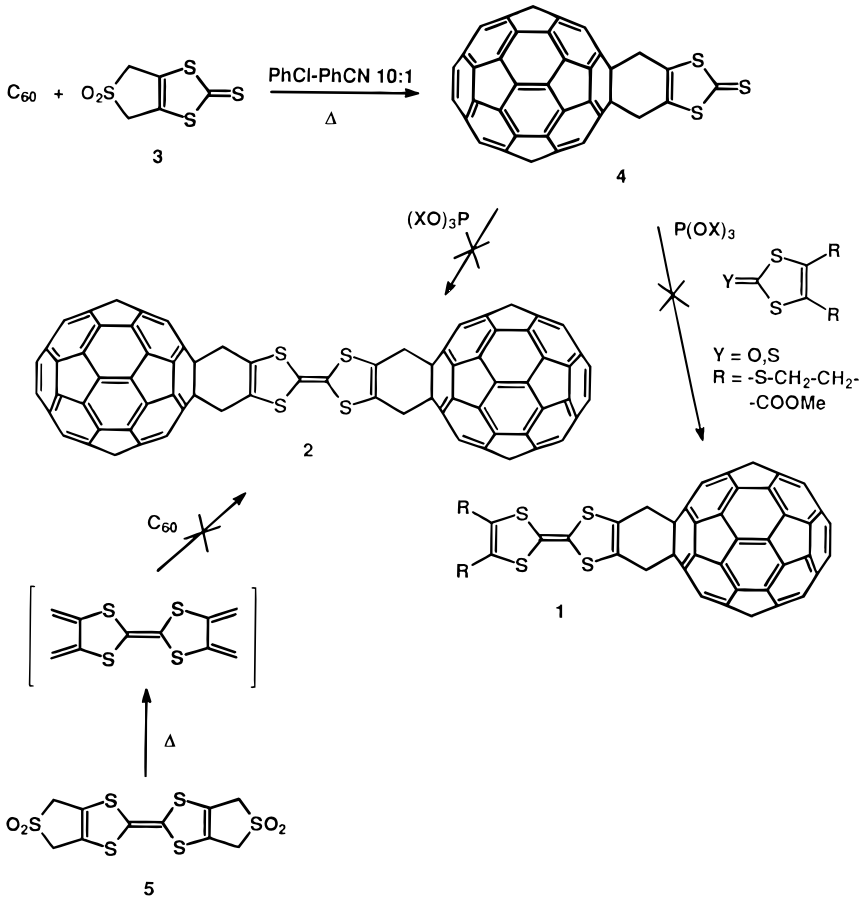

functional group offers a high chemical stability and is an excellent synthon of butadiene.[19,20]

We started with route I, and by direct cycloaddition to C_{60} of the diene formed in situ by thermal extrusion of sulfur dioxide from the 1,3-dithiole-2-thione **3** the cycloadduct **4** was obtained.[16]

Compound **4** appeared at this stage as a very promising precursor molecule to obtain, via a phosphite-mediated coupling,[18] the target compounds **1** and **2** (Scheme 2). Unfortunately, all attempts to perform such couplings failed.[16,21,22]

The lack of reactivity of compound **4** made us turn to the second approach (route II), outlined in Scheme 1, which is based on the construction of the TTF derivative bearing a labile 3-sulfolene group, and its subsequent cycloaddition to C_{60}. The first precursor that we tested was the tetrathiafulvalene derivative **5**,[23] which has double functionality, being the precursor of the target compound **2**. When the extremely insoluble tetrathiafulvalene **5** was refluxed in chlorobenzene or benzonitrile/*o*-dichlorobenzene mixtures with an excess of C_{60}, no clear evidence of the formation of compound **2** or of the recovery of the starting compound **3** in the reaction mixture was observed by chromatography (TLC and HPLC) and cyclic voltammetry. This result can be explained if the in situ-generated bis-butadiene TTF derivative gives rise to rapid polymerization, preventing its cycloaddition to C_{60}. To control the reactivity, we select the asymmetric TTF−diene precursors **6**, carrying one sulfolene group on one side and various substituents on the other side. Moreover, this synthetic pathway affords the possibility to prepare different cycloadducts with distinct substituents on the TTF moiety that would modify the electron-donor ability of the addend, expanding the scope of the physicochemical studies. On the basis of a Wittig methodology, we have developed a procedure that gave good results for the synthesis of the family of nonsymmetric TTF derivatives **6**.[24]

The first C_{60}−TTF dyad to be obtained in our laboratory was compound **1a**, bearing two electron-withdrawing groups in the TTF moiety.[16] Such a dyad as well as the other Diels−Alder cycloadducts **1b** and **1c** were prepared by refluxing for 1 h solutions of C_{60} and the corresponding diene precursors **6a**−**c** in a 2:1 ratio (Scheme 3). Reactions proceeded to give the monoadducts as major products, although in the coupling of **6a** the mixture of regiosomeric bisadducts **1d** was also obtained. Longer reaction times do not improve significantly the reaction yields.[25] Compound **1b** was also obtained in a low yield (12%) by an alternative reaction pathway consisting of

(19) Inomata, K.; Kinoshita, H.; Takemoto, H.; Murata, Y.; Kotake, H. *Bull. Chem. Soc. Jpn.* **1978**, *51*, 3341.

(20) Yamada, S.; Ohsawa, H.; Suzuki, T.; Takayama, H. *J. Org. Chem.* **1986**, *51*, 4934.

(21) Homocoupling attempts were carried out using various coupling agents, including neat trimethyl phosphite, triethyl phosphite, and triphenyl phosphite, as well as toluene/phosphite mixtures. Several 1,3-dithiole-2-chalcogen systems were also used in order to obtain dyads **1**, but the desired compounds were not detected in the reaction mixtures, and the starting compound **4** was always recovered almost quantitatively.

(22) Boulle, C.; Cariou, M.; Bainville, M.; Gorgues, A.; Hudhomme, P.; Orduna, J.; Garín, J. *Tetrahedron Lett.* **1996**, *38*, 81.

(23) Veciana, J.; Rovira, C.; Cowan, D. *Tetrahedron Lett.* **1988**, *29*, 3467.

(24) Llacay, J.; Mata, I.; Molins, E.; Rovira, C.; Veciana, J. *Adv. Mat.* **1998**, *3*, 330.

Scheme 3

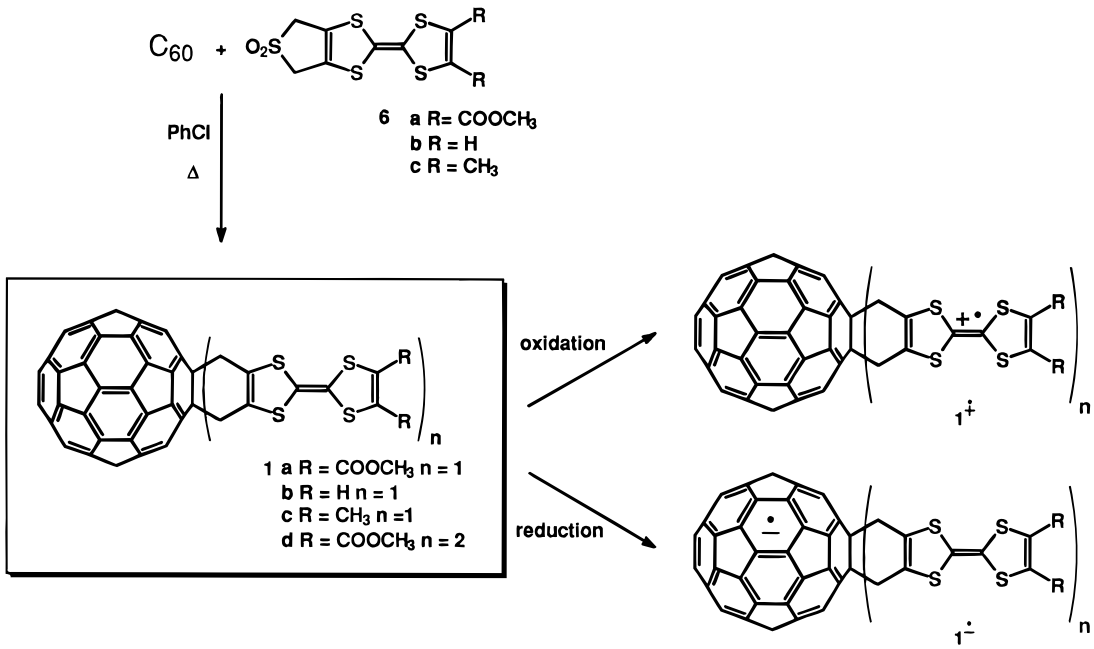

Table 1. Electronic Absorptions (λ, nm) of Dyads 1a−d and Their Radical-Cation and Radical-Anion Derivatives

compd	neutral species	radical cation	radical anion[c]
1a[a]	256, 313, 432, 700	314, 449, 610	1009, 889, 797
1b[a]	257, 312, 432, 699	315, 457, 617	
1c[b]	257, 312, 432, 700	317, 465, 658	
1d[a]	257	310, 449	

[a] In CH_2Cl_2. [b] In 1,1,1-trichloroethane. [c] In THF.

the thermal decarboxylation of **1a** in HMPA. DSC analysis of the adducts **1a**−**d** shows no decomposition processes from room temperature to 375 °C, revealing that the cycloadducts are very stable upon thermal treatment. Only a partial thermal decomposition above 280 °C was observed for compounds **1a** and **1d**, which was ascribed to the loss of the carboxymethyl groups attached to the TTF moiety. The structure of the Diels−Alder adducts **1a**−**d** was confirmed by their analytical and spectroscopic data. Comparing the ^{1}H NMR data of the family of cycloadducts **1** with the corresponding TTF precursors **6**,[24] the methylenic groups are downfield shifted when the sulfone group is replaced by C_{60}; on other hand, they do not show any dependence on the substituent attached to the TTF ring. The same phenomenon is observed in the characteristic electronic absorptions of dihydrofullerenes (Table 1),[26,27] since such absorptions appear at wavelengths that are virtually independent from the substituents of the TTF addend. Nevertheless, an interesting spectral feature is observed in these solution spectra for dyads **1a**−**c**. This is a weak broad band between 450 and 520 nm, which is absent in the reference adduct **4**. Similar broad bands have also been reported for other C_{60}-based dyads,[4,7b,26] and they have been ascribed to weak electronic interactions between donor and acceptor moieties. In accordance with this character, the ratio of intensities of the absorption band at 432 nm and the quoted band decreases with the donor strength of the TTF addend, the intensity ratios observed for compounds **1a**, **1b**, and **1c** being 9.6, 7.0, and 2.5, respectively.

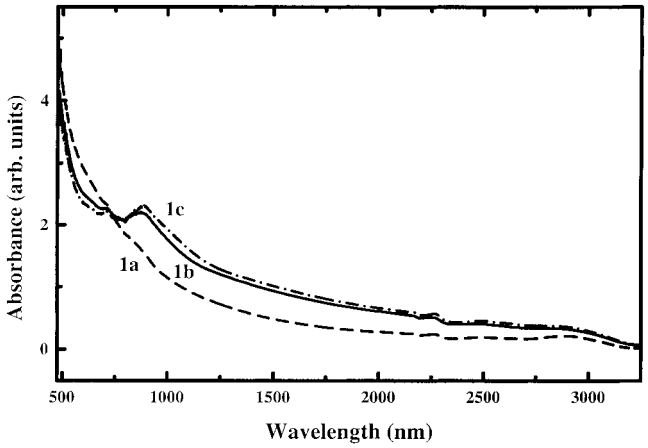

Figure 1. Vis-NIR spectra of C_{60}−TTF dyads in KBr disks.

To study if there is any degree of charge transfer in the solid state, the EPR and electronic spectra of solid samples of dyads **1a**−**c** were recorded. EPR of powder samples revealed only very weak signals that could not be clearly assigned to radical-ion species formed by such charge-transfer processes. Electronic absorption spectra of solid samples dispersed in KBr showed new bands, with respect to the spectra of TTF's **6** and C_{60}, at 886 and 947 nm for dyads **1b** and **1c**, respectively (Figure 1), while compound **1a**, with the poorest addend donor linked to C_{60}, did not present any absorption in this region. Such low-energy bands that were not present in the spectra obtained in solution are very similar to those observed in other solid neutral charge-transfer complexes

(25) Dyad **1a** was isolated as a crystalline solid by slow evaporation from concentrated CH_2Cl_2 solutions. Single crystals were not suitable for a complete X-ray analysis, and only cell parameters were determined: a = 10.12(2) Å, b = 12.87(21) Å, c = 17.10(10) Å; α = 98.28(95)°, β = 90.50(28)°, γ = 109.82(60)°, V = 2070 (37) Å^3. The electrical conductivity of single crystals was measured with the four-probes method, revealing an insulator (R > 20 MΩ) behavior. The growth of single crystals of dyads **1b** and **1c** turned out to be even more difficult than for dyad **1a**.

(26) Nakamura, Y.; Minowa, T.; Tobita, S.; Shizuka, H.; Nishimura, J. *J. Chem. Soc., Perkin Trans. 2* **1995**, 2351.

(27) Suzuki, T.; Maruyama, Y.; Akasaba, T.; Ando, W.; Kobayashi, K.; Nagase, S. *J. Am. Chem. Soc.* **1994**, *116*, 1359.

Table 2. $E_{1/2}$ Values in V (vs Fc^+/Fc, Reference Internal) of C_{60}, 1, 4, and 6 in 0.1 M Bu_4NPF_6 Solution at Room Temperature Using Pt as Working and Counter Electrodes

compd	solvent	$E_{+2/+1}$	$E_{+1/0}$	$E_{0/-1}$	$E_{-1/-2}$	$E_{-2/-3}$	$E_{-3/-4}$	ΔE_2[a]	ΔE_0[b]
C_{60}	CH_2Cl_2			−0.98	−1.36	−1.82			
	o-DCB			−1.11	−1.52	−1.99	−2.48		
4	CH_2Cl_2			−1.02	−1.39	−1.91			
	o-DCB			−1.16	−1.54	−2.06	−2.37		
1a[c]	CH_2Cl_2	0.69	0.21	−1.04	−1.43	−1.96		0.48	1.25
	o-DCB	0.65	0.13	−1.21	−1.63	−1.99	−2.57	0.52	1.34
1b	CH_2Cl_2	0.46	−0.04	−1.08	−1.47	−1.98		0.50	1.04
	o-DCB	0.43	−0.08	−1.17	−1.53	−2.05	−2.49	0.51	1.09
1c	CH_2Cl_2	0.41	−0.10	−1.08	−1.45	−1.96		0.51	0.98
	o-DCB	0.41	−0.15	−1.18	−1.55	−2.06	−2.52	0.56	1.03
1d	CH_2Cl_2	0.64	0.17	−1.16	−1.52	−1.95		0.47	1.33
	o-DCB	0.58	0.13	−1.27	−1.64	−2.02	−2.41[d]	0.45	1.40
6a[e]	CH_2Cl_2	0.68	0.35					0.33	
6b	CH_2Cl_2	0.48	0.16					0.32	
6c	CH_2Cl_2	0.49	0.07					0.42	

[a] $\Delta E_2 = E_{+2/+1} - E_{+1/0}$; difference between the first and second oxidation potentials. [b] $\Delta E_0 = E_{0/+1} - E_{0/-1}$; difference between the first oxidation and the first reduction potentials. [c] In *o*-DCB, an additional quasireversible wave is observed at −2.24 V. [d] Broad wave. [e] A quasireversible wave is observed at −1.72 V. *o*-DCB stands for *o*-dichlorobenzene.

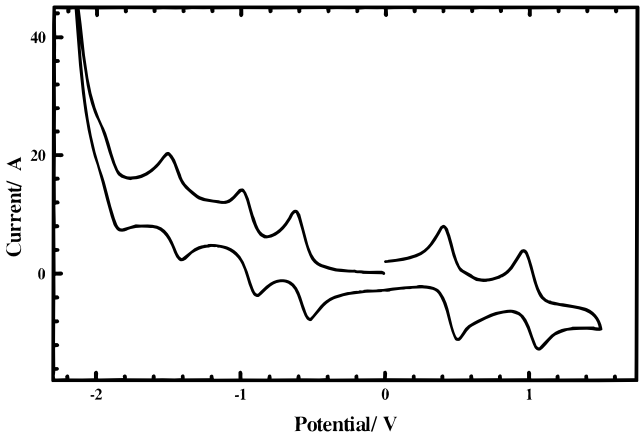

Figure 2. Cyclic voltammogram of dyad **1c** vs Ag^0/Ag^+. Conditions: 0.1 M, Bu_4NPF_6 in *o*-dichlorobenzene, 20 °C, 100 mV/s.

formed by C_{60} and TTF derivatives.[12,13] These bands have been assigned to a very small degree of intermolecular charge transfer arising from short intermolecular C···S contacts between the donors and the C_{60} molecule. In conclusion, the new bands observed in the electronic spectra in solid and solution states of cycloadducts **1b** and **1c** indicate the existence of weak inter- or intramolecular interactions between the donor and acceptor moieties.

Persistent Radical-Ion Derivatives. As expected from the bichromophoric nature of dyads **1a**−**d**, both oxidation and reduction processes were observed by cyclic voltammetry. Two reversible oxidation processes corresponding to the TTF's and up to three or four reversible reduction processes, depending on the solvent, due to the C_{60} are displayed (Table 2 and Figure 2). In addition, a quasireversible wave, arising from the carboxymethyl reduction, is observed between the third and fourth reduction processes for compounds **1a** and **1d**.

Reduction potentials are slightly shifted to more negative values with respect to C_{60}, as observed in other C_{60} cycloadducts,[28] and the observed values are invariant when changing the addend, revealing the absence of strong electronic interactions between the two chromophores. By contrast, oxidation potentials are more sensitive to the substituents of the TTF core. Thus, the

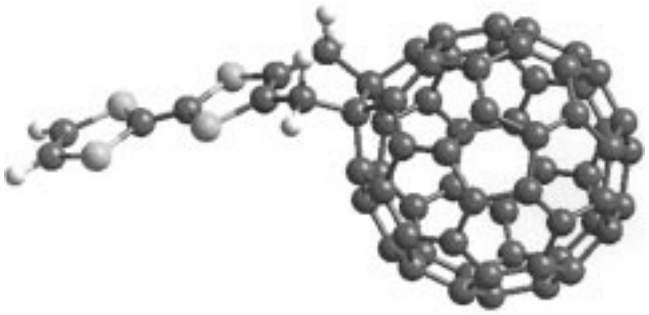

Figure 3. AM1-optimized structure of neutral dyad **1b**.

Table 3. Energies (in eV) of Frontier Orbitals of C_{60} and Cycloadducts 1a−c Obtained at the AM1 Level

compd	HOMO	LUMO	ΔE[a]
1[a]	−7.612	−2.883	4.729
1b	−7.285	−2.816	4.469
1c	−7.201	−2.800	4.401
C_{60}	−9.644	−2.947	6.697

[a] Difference between LUMO and HOMO energies.

gap between the first oxidation and the first reduction processes in these bichromophoric systems (ΔE_0 in Table 2) can be tuned by changing the electronic characteristics of the substituents of the TTF core. For example, the gap is 1.03 V in *o*-dichlorobenzene (0.98 V in methylene chloride) for the cycloadduct **1c**, bearing a methyl group, while for compound **1a**, with strong electron-withdrawing groups, the gap is 1.34 V (1.25 V in methylene chloride). It is interesting at this point to discuss the electrochemical results obtained with dyads **1a**−**c** in terms of the energy of their frontier orbitals. Optimized geometries (Figure 3) and the frontier orbital energies have been calculated for C_{60} and neutral dyads **1a**−**c** at the AM1 level. The trend in the HOMO energies of the new family of dyads is in agreement with that observed in the first oxidation potentials obtained by cyclic voltammetry (Table 3).

The presence on the same molecule of electron donor and acceptor moieties makes possible the generation of

(28) Chlistunoff, J.; Cliffel, D.; Bard, A. J. In *Handbook of Organic Conductive Molecules and Polymers*; Nalwa, H. S., Ed.; John Wiley & Sons Ltd.: New York, 1997; Vol. 1, Chapter 7.

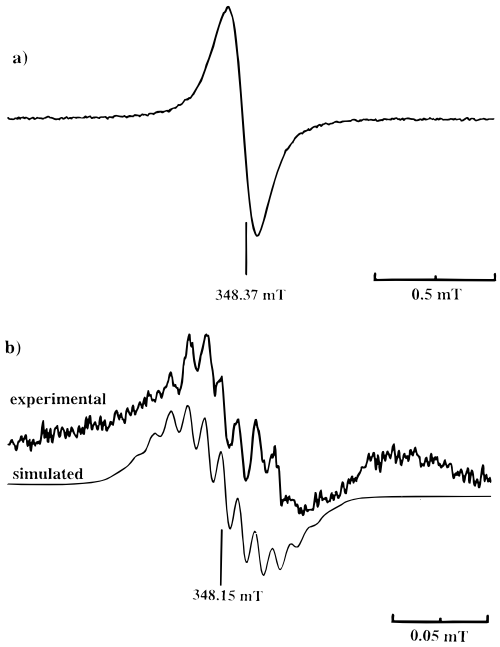

Figure 4. EPR spectra in CH_2Cl_2 at 295 K of radical anions derived from monoadduct **1a** (a) and bisadduct **1d** (b) as NBu_4^+ salts.

their radical-cation and radical-anion derivatives upon oxidation or reduction, respectively. Thus, the monoradical anions of cycloadducts **1a**−**c** were generated by electrochemical reduction and monitored by EPR spectroscopy. Such radical anions have large persistences with lifetimes of the order of days, showing under isotropic conditions (in CH_2Cl_2 solutions at 295 K) EPR spectra (Figure 4a) consisting of narrow symmetric doublets with no hyperfine structures, as observed in many other fullerides derived from C_{60} cycloadducts.[29−31] This result is in agreement with a spin density distribution mostly confined to the fullerene cage with only a very low spin density in the addend.[31]

As shown in Table 4, the *g* factors and peak-to-peak line widths of radical anions derived from cycloadducts **1a**−**c** do not show any dependence on the substituents of the addend being close to the values reported for pure $C_{60}^{\bullet-}$ and other fullerides.[31−33] As also observed for fullerides derived from other C_{60} cycloadducts, we do not detect the development of an additional second EPR line, which is present in underivatized $C_{60}^{\bullet-}$ under similar experimental conditions.[34]

The EPR spectrum of the radical anion derived from the bisadduct **1d** (mixture of regioisomers) (Figure 4b) contrasts with those of monoadducts previously described. Indeed, this radical anion shows a higher *g* factor and a narrower EPR signal, which permits observation of the hyperfine structure arising from the coupling of the unpaired electron with the hydrogen atoms of the methylenic groups of the bridges. The resulting structured signal of this radical anion is compatible with two sets of hydrogen atoms with small hyperfine coupling constants (around 0.0176 mT (4H) and 0.0085 mT (4H)), these small values being consistent with a low spin density on the addend. To our knowledge, this is the first example of a radical anion derived from a fullerene where the coupling of the unpaired electron with some atoms of the addend has been observed. A more complete study on the isolated isomers of **1d** is now being pursued in our laboratory.[35]

Table 4. EPR Data Corresponding to Persistent Open-Shell Species Derived Form C_{60}, 1, 4, and Related TTF Derivatives

	radical cation			radical anion	
compd	*g*	a_H (mT)	a_S (mT)	*g*	line width (mT)
1[a]	2.0077	0.196 (2H)	0.464 (2*S*)[a]	1.9997	0.118
			0.382 (2*S*)[a]		
1b	2.0077	0.119 (2H)[a]	0.412 (2*S*)[a]	1.9999	0.112
		0.149 (2H)[a]	0.435 (2*S*)[a]		
1c	2.0075	0.132 (2H)[a]	0.400 (4*S*)[a]	1.9996	0.128
		0.080 (6H)[a]			
1d	2.0077	0.202 (2H)[a]	*b*	2.0005[c]	0.063[c]
C_{60}				1.9998	0.102
4				1.9999	0.173
TTF[d]	2.0081	0.125 (4H)	0.425 (4*S*)		
TM-TTF[d]	2.0078	0.074 (12H)	0.395 (4*S*)		
TCM-TTF[e]	2.0081		0.452 (4*S*)		

[a] Values obtained by the computer simulation of experimental spectra. [b] Simulation not satisfactory. [c] Coupling with hydrogen atoms was observed under more accurate conditions (see text). [d] From ref 39. [e] From ref 47. TM-TTF and TCM-TTF stand for tetramethyl-TTF and tetracarboxymethyl-TTF, respectively.

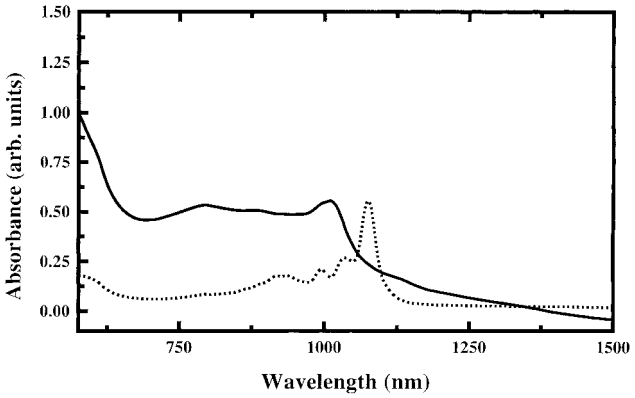

Figure 5. Vis-NIR spectra in THF solution of fullerides $\mathbf{1a}^{\bullet-}$ (solid) and $C_{60}^{\bullet-}$ (dashed) as NBu_4^+ salts.

UV−vis-NIR spectra of the monoradical anions generated electrochemically in THF, CH_2Cl_2, and benzonitrile were recorded but, due to the very low solubility of the starting compounds, a reliable spectrum was obtained only in THF for **1a**. As shown in Figure 5, its electronic spectrum exhibits the typical absorption pattern of fullerides in the NIR region, although λ_{max} is somewhat shifted to the blue (by ca. 65 nm) with respect to C_{60}^-,[32,36] The same results have been reported for other fullerides derived from C_{60} cycloadducts.[29,31]

(29) Brezová, V.; Gügel, A.; Rapta, P.; Stasko, A. *J. Phys. Chem.* **1996**, *100*, 16232.
(30) Jones, M. T.; Kadish, K. M.; Subramanian, R.; Boulas, P.; Vijayashree, M. N. *Synth. Met.* **1995**, *70*, 1341.
(31) (a) Sun, Y.; Drovetskaya, T.; Bolskar, R. D.; Bau, R.; Boyd, P. D. W.; Reed, C. A. *J. Org. Chem.* **1997**, *62*, 3642. (b) Baumgarten, M.; Ghergel, L. *Progress in Fullerene Research*; World Scientific: Singapore, 1994; pp 348−388.
(32) Baumgarten, M.; Gügel, A.; Ghergel, L. *Adv. Mater.* **1993**, 458.
(33) Khaled, M. M.; Carlin, R. T.; Trulove, P. C.; Eaton, G. R.; Eaton, S. S. *J. Am. Chem. Soc.* **1994**, *116*, 3465.
(34) Staško, A.; Brezová, V.; Biskupic, S.; Dinse, K.-P.; Schweitzer, P.; Baumgarten, M. *J. Phys. Chem.* **1995**, *99*, 8782.
(35) We are currently working in the isolation of pure regioisomers of **1d** in order to study the different spin density distribution resulting from the distinct substitution patterns.
(36) Baumgarten, M.; Ghergel, L. *Synth. Met.* **1995**, *70*, 1389.

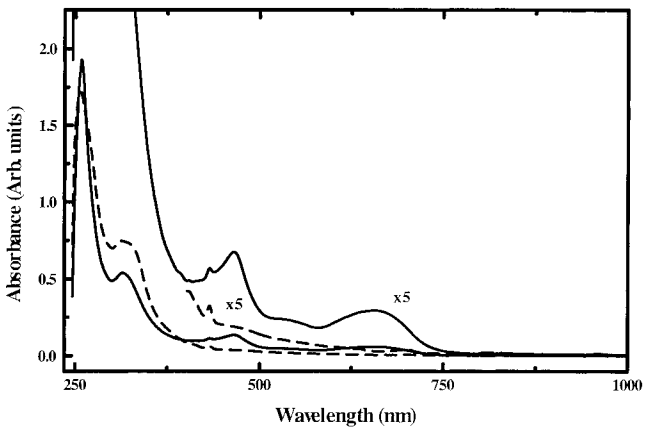

Figure 6. UV−vis spectra in CH_2Cl_2 of neutral dyad **1c** (dashed) and its radical-cation derivative **1c**$^{+\bullet}$ (solid) as the PF_6^- salt.

Radical cations of dyads **1a**−**d** were obtained by electrochemical oxidation and were characterized by EPR and electronic spectroscopies. Such radical cations show persistence in solution even larger than that of the corresponding radical anions described previously. The radical cations derived from **1a**−**c** show new bands in the 400−600 nm region (Figure 6), not present in the neutral molecules, and which are characteristic of radical cations centered on a TTF core (Table 1).[37,38] No bands above 700 nm were observed, indicating the absence in solution of any dimer formed through a π stacking of the TTF addends.[37] This fact is not surprising if we take into account the large steric hindrance introduced by the bulky fullerene cage and the poor solubilities of these compounds that prevent the preparation of highly concentrated solutions that usually favor such processes.

All radical-cation derivatives of this family of dyads exhibit multiplet EPR signals arising from the coupling of the unpaired electrons with the hydrogen atoms of the addend. Additional satellite lines, derived from the ^{33}S hyperfine interactions, are also observed upon enlargement of the signals as shown in Figure 7.

Hyperfine coupling constants obtained for ^{33}S and the *g* factors are given in Table 4, being typical of radical cations of TTF derivatives.[39] This result indicates that the unpaired electron is mainly localized on the TTF addend in such radical cations. Interestingly, the proton hyperfine structures of all radical cations show that only two of the four methylenic protons of the cyclohexene bridges between the C_{60} and the TTF addend have a significant coupling with the unpaired electron. This fact is illustrated in Figure 7 by the EPR spectrum of the radical cation derived from **1a**, where the central signal consists of a triplet arising from the coupling with only two equivalent protons of the two methylene groups. This result can be explained if the cyclohexene bridge adopts a quite rigid boat conformation fixing two different sets of two hydrogen atoms: *equatorial*, which are expected to be almost perpendicular to the TTF plane, and *axial*, which would lie practically in the plane of the TTF ring.[40] Consequently, the first two hydrogen atoms would be immersed inside the SOMO region of the radical cation and couple with the unpaired electron, while the other two hydrogen atoms would lie on the nodal plane of the SOMO showing a negligible hyperfine coupling constant. Therefore, the observation of significant coupling constants with only one pair of methylenic hydrogen atoms can be ascribed to the fact that the boat-to-boat interconversion takes place at a rate much lower than the EPR time-scale; i.e., the interconversion rate *k* is much lower than the difference between the *axial* and *equatorial* hyperfine coupling constants in frequency units ($k \ll 1 \times 10^6$ s^{-1}). This fact is in accordance with the high barrier to inversion of the boat conformation leading to slow boat-to-boat interconversion rates of $k \approx 1 \times 10^2$ s^{-1} found for other neutral cycloadducts of C_{60} with either carbocyclic[41] or heterocyclic *o*-quinodimethanes.[42]

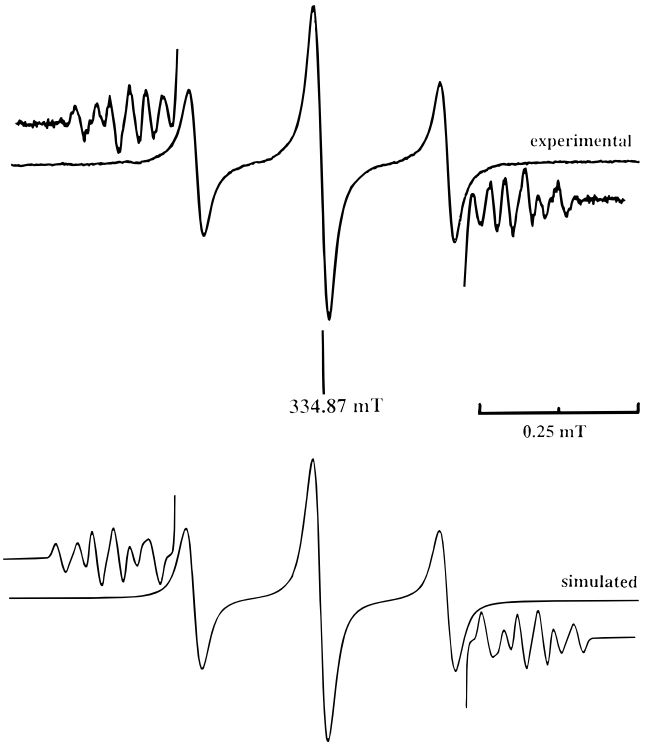

Figure 7. Experimental at 293 K and simulated EPR spectra in CH_2Cl_2 under isotropic conditions of the radical cation derived from dyad **1a** as PF_6^- salt. Amplified signals show the satellite lines due to the ^{33}S hyperfine couplings.

Transient Radical-Ion Derivatives. Having characterized the persistent open-shell species derived from dyads **1a**−**c** upon a monoelectronic transfer process, we started photophysical studies with these dyads in order to ascertain whether intramolecular electron-transfer

(37) Torrance, J. B.; Scott, B. A.; Welber, B.; Kaufman, F. B.; Seiden, P. E. *Phys. Rev. B* **1979**, *19*, 730.

(38) Talham, D. R.; Chou, L.-K.; Quijada, M. A.; Clevenger, M. B.; Oliveira, G. F. d.; Abboud, K. A.; Tanner, D. B. *Chem. Mater.* **1995**, *7*, 530.

(39) (a) Cavara, L.; Gerson, F.; Cowan, D. O.; Lerstrup, K. *Helv. Chim. Acta* **1986**, *69*, 141. (b) Rovira, C.; Veciana, J.; Santaló, N.; Tarrés, J.; Cirujeda, J.; Molins, E.; Llorca, J.; Espinosa, E. *J. Org. Chem.* **1994**, *59*, 3307.

(40) In fact, the AM1-optimized molecular geometries of **1a**−**c** dyads (Figure 3) have their cyclohexene rings adopting boat conformations with averaged angles between mean planes around 133° that are close to those found in the crystal structure of thione **4**.[16] These optimized geometries present two sets of hydrogen atoms; one set of two atoms forming an angle α of 13° between the C−H bond and the plane defined by the TTF core and the other set of two hydrogen atoms forming an angle β of 106°.

(41) (a) Rubin, Y.; Khan, S.; Freedberg, D. I.; Yeretzian, C. *J. Am. Chem. Soc.* **1993**, *115*, 344. (b) Tago, T.; Minowa, T.; Okada, Y.; Nishimura, J. *Tetrahedron Lett.* **1993**, *34*, 8461. (c) Zhang, X.; Foote, C. S. *J. Org. Chem.* **1994**, *59*, 5235.

(42) Fernández-Paniagua, U. M.; Illescas, B.; Martín, N.; Seoane, C.; Cruz, P.; Hoz, A.; Langa, F. *J. Org. Chem.* **1997**, *62*, 3705.

Chart 2

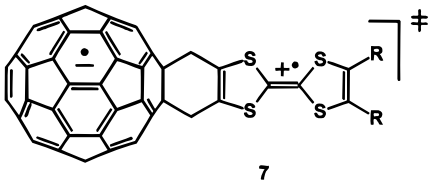

7

processes from the donor to the excited states of C_{60} could generate open-shell species with separated charges such as in **7** (Chart 2). As already mentioned, semiempirical AM1 calculations show that the LUMO energies of dyads **1** are almost independent of the TTF addend, the LUMOs being located exclusively on the C_{60} framework. By contrast, the HOMO energies depend on the TTF substituent, being mainly located in the TTF addend, although a small part is also located on the C_{60} framework. Consequently, the energy gap between LUMO and HOMO orbitals can be tuned by changing the electron-releasing or electron-withdrawing character of the substituents of the TTF addends. Therefore, these computational results indicate that dyad **1a**, which bears two strong electron-withdrawing groups on the TTF moiety, has a less favorable energy gap in order to exhibit an intramolecular electron-transfer phenomenon. On the contrary, compound **1c**, with moderate electron-releasing groups, is the most suitable dyad to produce such interactions.

Photoinduction of charge transfer has been studied by nanosecond-resolved flash photolysis in the UV−vis region. The cycloadduct **4** that does not have any TTF donor moiety has been used as a reference compound. The different transient absorption spectra of dyads **1a**−**c** and cycloadduct **4** have been recorded after irradiation of benzonitrile solutions with a 532 nm pulsed (9 ns) laser. As the TTF moiety is transparent to the 532 nm irradiation, we can expect that only the fullerene moiety is excited under such irradiation. All the samples show the initial formation of an excited triplet state with a spectral maximum at around 700 nm that deactivates monoexponentially at different rates depending on the substituent of the cycloadduct.[43] Whereas the model compound **4** behaves similarly to pristine C_{60}[8b] with a lifetime of $\tau = 25$ μs, the excited triplet states of dyads **1a**, **1b**, and **1c** are rapidly quenched with $\tau = 2.9$, 2.9, and 0.25 μs, respectively. This behavior can be accounted for by an extra quenching of the triplets due to an intramolecular charge transfer when the energy gap between of HOMO and LUMO decreases. Remarkably, dyad **1c** shows the fastest quenching rate, in accordance with the strongest donor ability of the TTF addend. While the triplet excited state is quenched, a second transient appears for dyads **1b** and **1c**, as shown in Figure 8. These second transients display absorption spectra with two bands centered around 460 and 620 nm that simultaneously decay monoexponentially at rates of $\tau = 75$ and 79 μs for **1b** and **1c**, respectively. For compound **1a**, this second transient species is not clearly observed. Interestingly, the spectra of this transient species have the same absorptions than those of the related radical cations electrochemically derived from **1b** and **1c** (see Figure 6).[44] This result provides, therefore, direct evidence of the generation of the charge-separated state formed upon a photoinduced intramolecular electron-transfer from the donor to the acceptor moiety in the bichromophoric cycloadducts **1b** and **1c**.

Definitive evidence of photoinduced electron transfer that generates long-lived charge-separated species was obtained from LEPR (light-induced electron paramagnetic resonance) experiments. Thus, steady-state EPR spectra of a glassy solution of dyads **1b** and **1c** in benzonitrile/CH_2Cl_2 (1:1) was recorded at 90 K before and after irradiation with the colimated beam from a mercury lamp (400 W). Upon irradiation, a broad signal appears for compounds **1b** and **1c** ($\Delta H = 12.5$ and 13.0 G, respectively), while no significant signal was observed for the dyad **1a**. These facts are in accordance with the results obtained by flash photolysis. When the temperature is raised to 180 K, the LEPR signal almost disappears, indicating a lower lifetime of the photoinduced species. The resulting EPR signals (Figure 9) have g values (**1b**, $g = 2.0039$; **1c**, $g = 2.0037$) that are intermediate between those shown by the corresponding radical cations **1b**$^{\bullet+}$ and **1c**$^{\bullet+}$ and radical anions **1b**$^{\bullet-}$ and **1c**$^{\bullet-}$ generated electrochemically (see Table 4). This averaging of the g factor is a consequence of an effective exchange interaction $J(S_1 \cdot S_2)$ between the two electrons of the triplet charge-separated species. The shape of the EPR signals of these charge-separated species in rigid glass matrixes are consistent with small zero-field splitting parameters ($D \leq 15$ G and $E = 0$ G), in accordance with a large separation of the two interacting electrons if it is assumed that the highest spin density for the anion radical is mostly confined in the equatorial region of C_{60}.[31a] This result is in agreement with a previous one on biradical anions of fulleropyrrolidines substituted by nitroxide radicals.[45]

Conclusions

In summary, a new family of donor−acceptor-fused dyads derived from C_{60} and TTF has been synthesized and studied. These new compounds have a short and rigid bridge between TTF and C_{60} that allows the appearance of a weak interaction between both electroactive moieties, as ascertained by electronic absorption spectroscopy. The introduction of different functional groups in the TTF addend allows the tuning of the energy gap between the frontier orbitals of the dyads, which have important consequences on their electrochemical and photophysical properties. Remarkable is the evidence provided about the tuning of the lifetime of the excited triplet state by modifying the donor ability of the TTF addend. In addition, the long lifetime of the transient charge-separated open-shell species formed is particularly interesting. A deeper study of the photphysical properties of dyads **1** will be performed. Both radical cations and radical anions derived from these dyads have been obtained and characterized and display outstanding persistences. Their stability encourages the synthesis of solid radical-ion salts; this objective is currently being approached in our laboratory.

(43) Along with this maximum, another one was also observed around 390 nm with a lower abosrbance that deactivates exponentially at the same rate as the first maximum for all the studied dyads.

(44) The characteristic band of $C_{60}^{\bullet-}$ expected at around 1010 nm for these charge-separated species lies outside the limit of our detector.

(45) Arena, F.; Bullo, F.; Conti, F.; Corvaja, C. Maggini, M.; Prato, M.; Scorrano, G. *J. Am. Chem. Soc.* **1997**, *119*, 789.

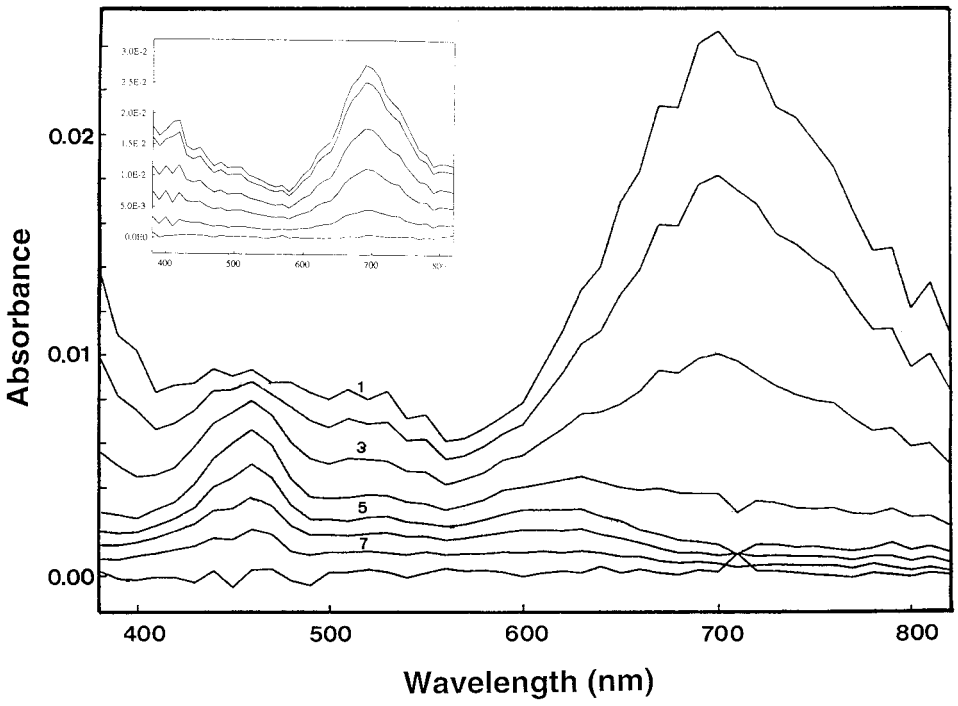

Figure 8. Transient absorption spectra at different times obtained by laser flash photolysis of 0.1 mM solutions of **1b** in benzonitrile after a 532 nm pulsed (9 ns) laser excitation. Times after pulse: (1) 2×10^{-6} s; (2) 4×10^{-6} s; (3) 8×10^{-6} s; (4) 1.6×10^{-5} s; (5) 3.2×10^{-5}; (6) 6.4×10^{-5}; (7) 1.3×10^{-4} s; (8) 2.5×10^{-4} s. Inset shows the corresponding spectra of thione **4** in the same conditions.

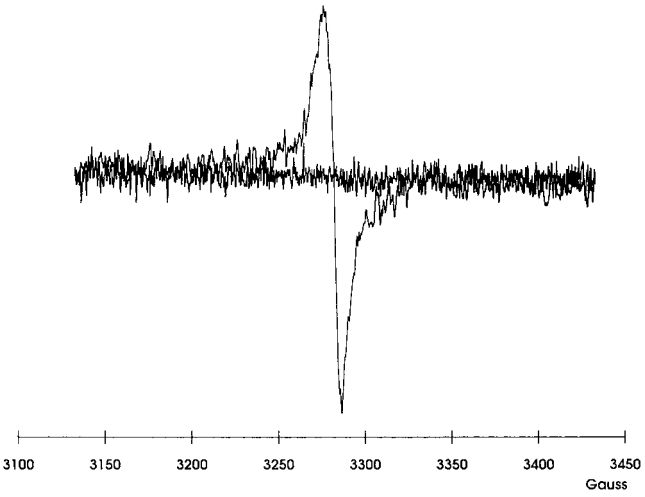

Figure 9. EPR spectra of dyad **1b** in glassy matrix (C_6H_6-CN:CH_2Cl_2, 1:1) at 90 K in the dark and after illumination.

Experimental Section

General Procedures. All cycloaddition reactions were performed under inert atmosphere and in the absence of light. C_{60} was purchased from MER corporation (Tucson, AZ). Cycloaddtions to fullerenes were monitored by thin-layer chromatography using Merck precoated silica gel 60-F_{254}. All the given yields are based on reacted C_{60}. Compounds **3**−**6** were prepared as described in the literature.[16,23,24]

Instruments. FT-IR spectra were recorded on a Nicolet 710 spectrophotometer on KBr disks. ^{1}H NMR and ^{13}C NMR spectra were taken on a Bruker AC 400 and a Bruker Aspect 3000 apparatus. UV−vis-NIR absorption spectra were obtained on a Varian Cary 5 spectrophotometer. EPR spectra were recorded on an X-Band spectrophotometer Bruker ESP 300 E, equipped with a temperature controller ER 412HT, a field frequency (F/F) lock accessory, and a built-in NMR gaussmeter; for LEPR experiments, an optical ER4104OR cavity and an Oriel set up with a mercury arc lamp of 400 W and a optic fiber were used. Thermal analyses were carried out on a Perkin-Elmer DSC 7 and a Perkin-Elmer TGA 7. FAB mass spectra were obtained on a VG TS-250 model, using 3-nitrobenzyl alcohol (NBA) as a matrix, and the MALDI mass spectra were obtained in time-of-flight positive linear mode on a Kratos Kompact Maldi 2 K-probe (KRATOS Analytical) operating with pulsed extraction of the ions. Cyclic voltammetries were carried out with an EG & G PAR 263A potentiostat/galvanostat on a cell equipped with a double KCl (3M) bridge, using the following working conditions: Pt wire, Ag/AgCl as a reference electrode, scanning rate 50−200 mV/s and Bu_4NPF_6 as a supporting electrolyte. Laser flash photolysis experiments were performed using a LKS50 instrument from Applied Photophysics. The second harmonic (532 nm) of a Q-switched Nd:YAG laser (Spectron Laser Systems, UK; pulse width ca. 9 ns) was used for the laser flash excitations. Typically, 17−25 mJ/pulse were used for sample excitation. The minimum-energy structures for dyads **1a**−**c**, **4**, and pristine C_{60} were calculated using the MOPAC 93 program running the AM1 Hamiltonian.[46]

Cycloaddition of C_{60} to the Diene Derived from 5,5-Dioxo-1,3-dithiole-2-thione. Compound 4. To a refluxing solution of 720 mg (1 mmol) of C_{60} in 150 mL of chlorobenzene was slowly added a solution of 112 mg (0.5 mmol) of thione **3** in 15 mL of anhydrous benzonitrile, and the resulting mixture was refluxed for 2 h. The solvent was evaporated, and the residue was purified by liquid chromatography (silicagel, CS_2−hexane), affording unreacted C_{60} (439 mg, 61%) and the monoadduct **4** as an inclusion compound with CS_2. The heating (120 °C) of the inclusion compound for 10 h under high vacuum afforded 139 mg (41%) of the solvent free thione **4**, isolated as a brown powder: FT-IR (KBr) ν (cm^{-1}) 1426, 1184, 1086, 1050, 766, 746, 696, 575, 553, 526, 508; ^{1}H NMR (300 MHz, $CDCl_3$) δ (ppm) 4.56 (s, 4H); ^{13}C NMR (75.5 MHz, CS_2−$CDCl_3$ 1:1, $Cr(acac)_3$) δ (ppm) 219.25, 154.05, 147.53, 146.28,

(46) For a semiempirical AM1 method, see: Dewar, M. J. S.; Zoebisch, E. G.; Healey, E. F.; Stewart, J. J. P. *J. Am. Chem. Soc.* **1985**, *107*, 3902. For MOPAC 93, see: Stewart, J. J. P. *MOPAC 93*; Fujitsu Limited: Tokyo, Japan, 1993.

(47) Terahara, A.; Ohya-Nishiguchi, H.; Hirota, N.; Awaji, H.; Kawase, T.; Yoneda, S.; Sugimoto, T.; Yoshida, Z.-i. *Bull. Chem. Soc. Jpn.* **1984**, *57*, 1760.

145.98, 145.33, 145.20, 144.61, 144.28, 143.87, 142.71, 142.36, 141.77, 141.36, 139.97, 138.24, 135.42, 128.54 (C_{sp2}), 64.50 (C_{60} C_{sp3}), 40.33 (CH_2); MS-FAB *m*/*z* 720 (100), 880 ($C_{65}H_4S_3$, 6.7); UV−vis (CH_2Cl_2) λ_{max} (log ϵ) 257 (5.02), 316 (4.41), 383 (4.41), 433 (3.58). Anal. Calcd for $C_{65}H_4S_3$: C, 88.63; H, 0.45; S, 10.90. Found: C, 88.09; H, 0.45; S, 10.76.

1,2-(Cyclohexenylbiscarboxymethyltetrathiafulvalene)-buckminsterfullerene Derivatives. Compounds 1a and 1d. To a refluxing solution of 144 mg (0.2 mmol) of C_{60} in toluene was added a solution of 41 mg (0.1 mmol) of compound **6a** in 8 mL of benzonitrile, and the resulting solution was refluxed for 1 h. The solvent was evaporated and the residue chromatographed (silica gel, CS_2−CH_2Cl_2) to give unreacted C_{60} (85 mg, 59.5%), 50 mg of monoadduct **1a** (58%), isolated as black microcrystalline needles, and 18 mg of a mixture of bisadducts **1d** (15.4%), isolated as a brown powder. **Adduct 1a**: FT-IR (KBr) ν (cm^{-1}) 1728, 1573, 1430, 1252, 1185, 1089, 1024, 754,695, 575, 527; ^{1}H NMR (300 MHz, CS_2−$CDCl_3$ 1:1) δ (ppm) 4.37 (s, 4H, CH_2), 3.89 (s, 6H, CH_3); ^{13}C NMR (75.5 MHz, CS_2−$CDCl_3$ 1:1) δ (ppm) 159.80 (C═O), 155.04, 147.80, 146.64, 146.36, 145.81, 145.67, 145.59, 144.97, 144.71, 143.20, 142.78, 142.30, 142.16, 141.73, 140.34, 135.85, 133.28 (C_{sp2}), 125.40 (C_{sp2}), 65.95 (C_{60} C_{sp3}), 53.25 (CH_3), 41.06 (CH_2); MS-FAB *m*/*z* 316 (100), 720 (80), 1066 ($C_{72}H_{10}O_4S_4$, 17); MALDI-MS 1066 [M^+]; UV−vis (CH_3CCl_3) λ_{max} (log ϵ) 256 (4.91), 313 (4.56), 432 (3.65), 700 (2.98). Anal. Calcd for $C_{72}H_{10}S_4O_4$: C, 81.05; H, 0.95; S, 12.0. Found: C, 80.99; H, 1.12; S, 11.89. **Bisadduct 1d**: FT-IR (KBr) ν (cm^{-1}) 1734, 1576, 1433, 1258, 1090, 1026, 766, 527; ^{1}H NMR (300 MHz, CS_2−CD_2Cl_2 1:2) δ (ppm) 4.31−4.25 (m, broad), 3.91−3.87 (m); HRMS calcd for $C_{84}H_{20}O_8S_8$ *m*/*z* 1411.892, found 1411.892; MALDI-MS 1412 [M^+]; UV−vis (CH_2Cl_2) λ_{max} (log ϵ) 257 (4.96), 310 sh.

1,2-(Cyclohexenyltetrathiafulvalene)buckminsterfullerene (1b). (a) From Cycloadduct 1a. To a solution of 56 mg (0.053 mmol) of compound **1a** in 6 mL of hexamethylphosphoramide (HMPA) was added 52 mg of LiBr (0.6 mmol). The resulting solution was kept for 15 min at 80 °C and then heated to 160 °C and kept at that temperature for 15 min. After cooling, 10 mL of water was added, the aqueous suspension was extracted with CS_2, and the organic layer was separated and dried with $NaSO_4$. The final solution was filtered over silica gel and evaporated to yield 6 mg (12.5%) of a brown powder characterized as compound **1b**.

(b) From C_{60} and Compound 6b. A solution of 289 mg (0.4 mmol) of C_{60} and 58 mg (0.2 mmol) of compound **6b** in 90 mL of chlorobenzene was refluxed for 1 h. The solvent was evaporated and the residue chromatographed (silica gel, CS_2−hexane) to give unreacted C_{60} (159 mg, 55%), several fractions of compound **1b** impurified with C_{60}, and 44 mg of pure compound **1b** (26%) isolated as a brown powder: FT-IR (KBr) ν (cm^{-1}) 1426, 1213, 1182, 796, 767, 637, 575, 553, 527, 510; ^{1}H NMR (300 MHz, CS_2−*o*-dichlorobenzene-d_4) δ (ppm) 6.34 (s, 2H), 4.32 (s, 4H); MS-FAB *m*/*z* 720 (100), 950 ($C_{68}H_6S_4$, 8); MALDI-MS 951 [$(M + H)^+$]; UV−vis (CCl_3CH_3) λ_{max} (log ϵ) 257 (4.92), 312 (4.54), 432 (3.63), 699 (3.11). Anal. Calcd for $C_{68}H_6S_4$: C, 85.88; H, 0.64; S, 13.48. Found: C, 85.81; H, 0.47; S, 13.49.

1,2-(Cyclohexenylbismethyltetrathiafulvalene)buckminsterfullerene (1c). A solution of 435 mg (0.6 mmol) of C_{60} and 96 mg (0.3 mmol) of compound **6c** was refluxed in 95 mL of chlorobenzene for 1 h. The solvent was evaporated and the residue chromatographed (silica gel, CS_2−hexane) to give unreacted C_{60} (270, 62%), several fractions of compound **1c** impurified with C_{60}, and 56.6 mg of pure compound **1c** (19%), isolated as a brown powder: FT-IR (KBr) ν (cm^{-1}) 1427, 1212, 1182, 1087, 766, 696, 575, 555, 527; ^{1}H NMR (300 MHz, *o*-dichlorobenzene-d_4) δ (ppm) 4.36 (s, 4H), 1.98 (s, 6H); ^{13}C NMR (75.5 MHz, *o*-dichlorobenzene-d_4) δ (ppm) 155.15, 147, 45, 146.33, 146.02, 145.30, 145.26, 144.81, 144.42, 142.84, 142.38, 142.06, 141.88, 141.40, 140.01, 135.54, 126.35 (C_{sp2}), 66.15 (C_{60} C_{sp3}), 40.87, 14.32; MS-FAB *m*/*z* 720 (100), 979 ($C_{70}H_{10}S_4$, 35); MALDI-MS 979 [$(M + H)^+$]; UV−vis (CCl_3CH_3) λ_{max} (log ϵ) 257 (4.74), 312 (4.38), 432 (3.32), 700 (2.48). Anal. Calcd for $C_{70}H_{10}S_4$: C, 85.87; H, 1.03; S, 13.10. Found: C, 84.60; H, 0.96; S, 13.10.

Generation of Radical Cations and Radical Anions Derived from 1a−d. Radical cations were obtained by in situ electrochemical reduction, monitored by an EG & G PAR 263A potentiostat/galvanostat, on an EPR cell equipped with Pt wires as working and counter electrodes and using the Ag/AgCl system as a reference electrode. Experimental conditions for the generation of radical cations were as follows: +0.7 V, CH_2Cl_2 0.2 M in Bu_4NPF_6. Experimental conditions for the generation of the radical anions of dyads **1a**−**d** were as follows: −0.8 V, CH_2Cl_2 0.2 M in Bu_4NPF_6.

Acknowledgment. This work was supported by grants from the Programa Nacional de Química Fina, (CIRIT-CICyT, Grant No. QFN93-4510-C01), DGICyT (Grant No. PB96-0872-c02-01) and by the Generalitat de Catalunya (Grant No. SGR95-507). J.L. thanks the CIRIT for a fellowship. The authors thank Dr. D. Powell (University of Florida, Gainsville, FL) for the HRMS data, M. Mas for the MALDI data, Dr. Vladimir Laukhin for the conductivity measurements, and J. Sedó for his helpful discussions about AM1 calculations.

JO980498B